



comes significantly larger as the system goes through  $T_V$ . In order to help interpret our measurements, we report extensive computations of the magnetic momentum density within the first-principles band theory framework. These and other model computations enable us to deduce that the anisotropy of the MCS provides a handle for ascertaining the localized vs delocalized nature of the magnetic electrons in the ground state of magnetite.

In an MCS experiment one measures the magnetic Compton profile (MCP),  $J_{\text{mag}}(p_z)$ , form momentum transfer along the scattering vector  $p_z$ , which is defined by

$$J_{\text{mag}}(p_z) = J_{\uparrow}(p_z) - J_{\downarrow}(p_z); \quad (1)$$

where  $J_{\uparrow}$  ( $J_{\downarrow}$ ) is the majority (minority) spin Compton profile.  $J_{\text{mag}}$  can be expressed in terms of a double integral of the spin density,  $m_{\text{ag}}(\mathbf{p})$ :

$$J_{\text{mag}}(p_z) = \int \int m_{\text{ag}}(\mathbf{p}) dp_x dp_y; \quad (2)$$

where  $m_{\text{ag}}(\mathbf{p}) = m_{\uparrow}(\mathbf{p}) - m_{\downarrow}(\mathbf{p})$  is the difference of the majority and minority spin densities. We emphasize that the area under  $J_{\text{mag}}(p_z)$  gives the spin moment  $s$ . In contrast, the information about the nature of the ground state wavefunction is described by the shape of  $J_{\text{mag}}(p_z)$ .

Experiments were performed on beam line 11-B at the Advanced Photon Source [18] using an elliptical multipole wiggler to generate circularly polarized photons. A high quality single crystal of  $\text{Fe}_3\text{O}_4$  was used and MCPs were measured along the [100] and [110] crystal directions at temperatures of 10 K, 100 K, 140 K, and 300 K. The Verwey transition temperature of the sample was determined via resistivity measurements to be  $120 \pm 1$  K. The incident photon energy was 125 keV. The scattering angle was  $170^\circ$ . All measurements were made under an external magnetic field of 7 T oriented along the direction of the scattering vector. The momentum resolution is estimated to be 0.4 a.u. (full-width-at-half-maximum). Magnetic calibration measurements [18] were performed using a crystal of Fe oriented along [110].

The electronic structure was computed for the high temperature (Fd3m) phase of  $\text{Fe}_3\text{O}_4$  within an all-electron, fully charge and spin self-consistent LDA-based band theory framework [19]. All computations were carried out to a high degree of accuracy, e.g., the crystal potential was converged to better than  $10^{-5}$  Ry. Our band structure is in good overall accord with the few available studies [8, 9, 10]. Various calculations agree on a half-metallic ferromagnetic band structure with the Fermi level crossing the minority spin  $t_{2g}$  bands originating from the octahedral Fe sites. The computed band structure and wavefunctions were used to obtain spin-resolved momentum densities  $m_{\uparrow}(\mathbf{p})$  and  $m_{\downarrow}(\mathbf{p})$ . These quantities were computed over a fine mesh of  $855 \times 10^6$  points within a sphere of radius 13 a.u. in  $\mathbf{p}$  space [20] in order to properly account for the fine structure

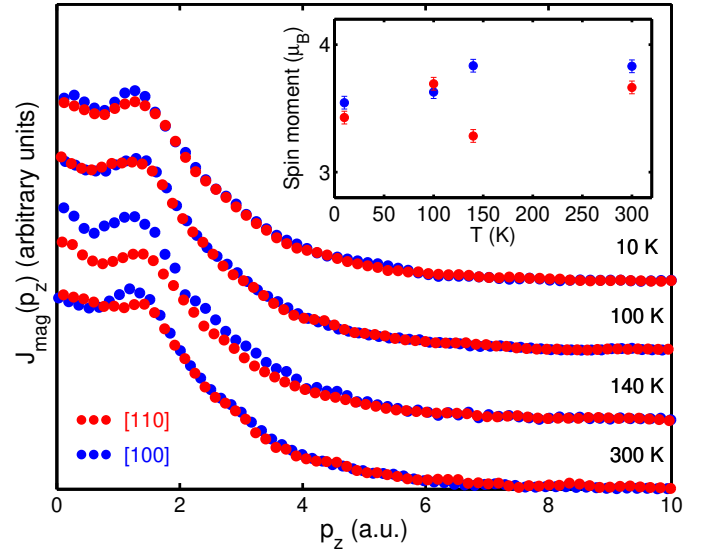


FIG. 1: (Color online)  $J_{\text{mag}}(p_z)$  for  $p_z$  along [100] (blue dots) and [110] (red dots) as a function of temperature. Different datasets are offset vertically with respect to one another. Symbol size is representative of error bars. Inset gives the magnetic moment of unpaired spins (per formula unit) obtained from the area under the MCP [11].

in  $\uparrow$  and  $\downarrow$ , and provided the dataset from which various projections of the spin-resolved momentum density and the MCPs along the high symmetry directions were computed.

The experimental spectra are summarized in Fig. 1. The area under the MCPs yields the magnetic moment  $s$  associated with uncompensated electronic spins shown in the inset.  $s$  has a value of  $3.54 \mu_B$ /formula unit at 10 K for the magnetic field along [100]. The uncertainty in  $s$  is estimated to be  $0.05 \mu_B$ . By comparing with the bulk magnetic moment of  $4.05 \mu_B$  [21], this yields a corresponding orbital component of  $0.51 \pm 0.05 \mu_B$ . Interestingly, the 140 K dataset near the Verwey transition displays a striking anomaly in that  $s$  is  $3.83 \mu_B$  when the 7 T field is along [100], but for the field along [110] it is  $3.28 \mu_B$ . This directional preference of  $s$  weakens again at higher temperatures.

It is interesting to note that  $s$  is non-integral. A simple ionic picture gives  $s = 4 \mu_B$  per formula unit [4]. In general, band theory can accommodate non-integral  $s$  since bands can be occupied partially. But, if spin is assumed to be a good quantum number, it is straightforwardly argued that  $s$  in a half-metallic system must also be strictly integral. However, a non-integral  $s$  value can be obtained if the spin-polarized band calculation is supplemented by spin-orbit interactions. The spin-orbit coupling has been estimated to be of the order of 10 meV [22], so that we would expect a substantial orbital moment due to  $\text{Fe}^{2+}$ .

Bulk magnetization measurements in magnetite [23, 24] reveal a significant magneto-crystalline anisotropy. This anisotropy is relatively small above  $T_V$  with [111] being the easy axis, while below  $T_V$ , the anisotropy is larger with [001] being the easy axis. However, the maximum saturation field is about 2T, so that under the field of 7T used in the present measurements, we would not normally expect anisotropic effects. Therefore, changes in the spin moment with the direction of the magnetic field seen in the inset to Fig. 1, which are especially striking at 140K, are anomalous and do not fit within the standard picture. The origin of this anomaly is unclear, but it may be related to the effect of geometrical frustration on magnetic properties above  $T_V$  [7]. Notably, Ref. [25] considers a Hamiltonian for the pyrochlore B lattice with a spin-orbit interaction. In this model, several complex orbital ordered states with noncollinear orbital moments are found as a possible ground state for the high-temperature phase. This degeneracy of the lowest energy states can be broken by an external magnetic field in a manner which depends on the field direction. Since the energy differences between these states are very small, a magnetic field of 7T can be sufficient to switch between the states [26]. Further MCS measurements of the spin moment in magnetite over a range of temperatures around  $T_V$  should prove worthwhile in this connection. Here a note should also be made of the role of magnons, which will reduce the moment below the canonical value of  $4 \mu_B$  at high temperatures [27].

Some insight into the shape of the MCPs can be obtained through the LDA-based first-principles band theory computations. This is illustrated in Fig. 2, which shows a good level of agreement between the shapes of the computed and measured [110] MCPs. The LDA correctly reproduces the overall width of the measured MCP as well as the pronounced peak at 1.3 a.u. The shallow bumps in the experimental MCP at momenta between 2–3 a.u. and 4–5 a.u. are similar to features in the theoretical MCP. This fine structure is the hallmark of interference terms that cannot be explained within a purely atomic picture.

In order to extract wavefunction localization features, we now discuss the anisotropy of the MCP defined as the difference between the two directional MCPs [28],

$$J_{\text{mag}} = \frac{D}{E} J_{\text{mag}}^{[100]} - J_{\text{mag}}^{[110]}, \quad (3)$$

where the brackets  $\langle \dots \rangle$  denote an average over temperature.  $J_{\text{mag}}^{[100]}$  is normalized at each temperature to the integral of the corresponding  $J_{\text{mag}}^{[110]}$ , so that  $J_{\text{mag}}$  integrates to zero. The average  $J_{\text{mag}}^{[100]}$  provides a temperature-independent "background" for highlighting changes in the shape of  $J_{\text{mag}}^{[110]}$  as a function of temperature. [29]

Fig. 3, which focuses on the 140K and 300K data above

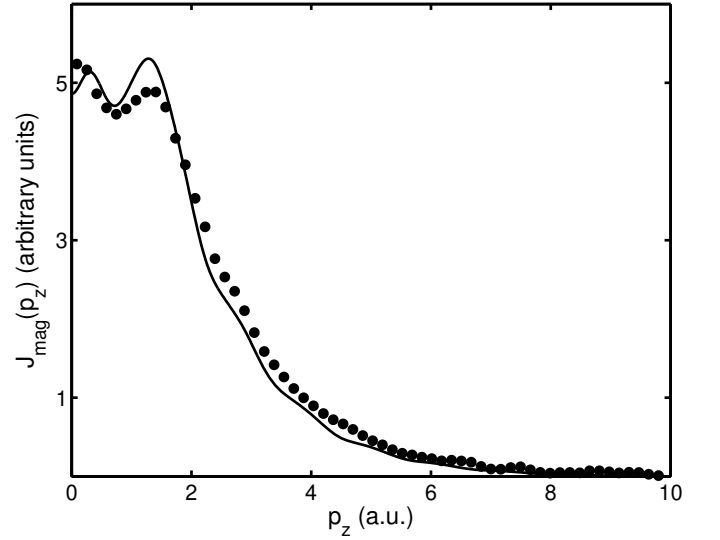


FIG. 2: Shape of the 140K [110] experimental MCP of Fig. 1 is compared with corresponding theoretical (resolution broadened) MCP obtained within the conventional LDA-based band theory framework.

the Verwey transition, shows that although the LDA reproduces the overall features in the measured anisotropy, the amplitude of the anisotropy given by the LDA is too large by about a factor of 4 (note that plotted LDA curve is scaled down). In order to gain insight into the shape and amplitude of  $J_{\text{mag}}$ , we have considered this quantity for a variety of clusters of Fe A- and B-site atoms and their nearest neighbor (NN) Fe atoms, using linear combinations of Slater type orbitals (STOs) where the cluster wavefunction is constructed by allowing STOs on NN Fe atoms to mix via a small admixture parameter  $f$  [30]. Our results show that the shape of the experimental

$J_{\text{mag}}$ , including the location of the peak at 1.12 a.u., can only be reproduced for a B-site Fe cluster in which the NN Fe atoms are situated at a NN distance  $d_{BB} = 5.61$  a.u. (2.97 Å) along the [110] direction [31]. In this case, the momentum wavefunction obtained by Fourier transforming the cluster wavefunction contains an oscillating factor of  $[1 + 2f \cos f d_{BB} (p_x + p_y) = \sqrt{2}g]$ , which yields the correct shape, and as Fig. 3 shows, for  $f = 0.1$  the computed curve (dashed) gives a good agreement in shape and amplitude with the 140K and 300K measurements in the low momentum region. We note that  $J_{\text{mag}}$  is rather insensitive to the inclusion of covalency with O atoms, and furthermore, the lack of oscillations in the cluster model at  $p_z > 2$  a.u. is related to inaccuracy in our STOs near the nucleus and is of little interest in the present context of solid state effects.

In order to delineate the temperature dependence of  $J_{\text{mag}}$  the results for the 10K and 100K datasets below  $T_V$  are presented in Fig. 4. The peak located at

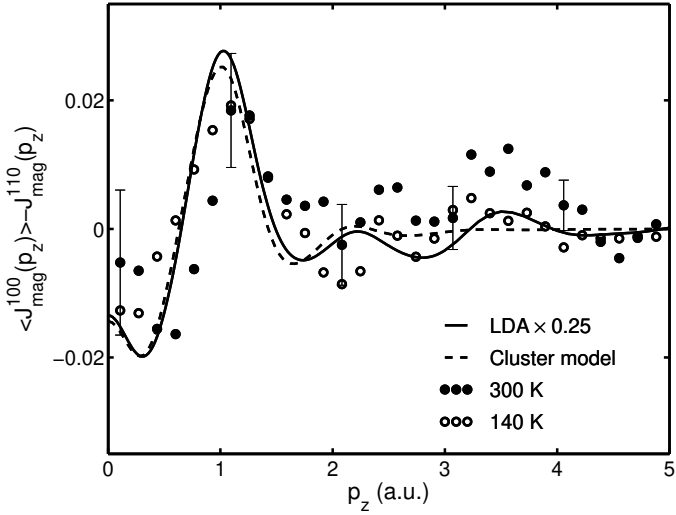


FIG. 3: Anisotropy of the MCP defined as  $J_{\text{mag}} = \frac{J_{\text{mag}}^{[100]} - J_{\text{mag}}^{[110]}}{J_{\text{mag}}^{[100]} + J_{\text{mag}}^{[110]}}$ , where the areas under all profiles are normalized to one. Experimental results for the 140K and 300K datasets are compared with the anisotropy obtained within the conventional LDA-based band theory framework and the model cluster computation discussed in the text. Note, the LDA curve has been scaled down by a factor of 4.

1.12 a.u. is seen now to have essentially disappeared and the anisotropy is strongly reduced compared to even the scaled LDA curve. The rather flat result of Fig. 4 is consistent with a value of the admixture parameter  $f = 0$  [32] and with the simple atomic analysis of Ref. [17]. A similar result for  $f$  was obtained from an analysis of a positron annihilation study on magnetite carried out below  $T_V$  [30].

To be more quantitative we define the anisotropy amplitude

$$A = \frac{1}{2} \int_0^{p_{\text{max}}} J_{\text{mag}}(p) dp; \quad (4)$$

where  $p_{\text{max}} = 5$  a.u. is a momentum cutoff [3]. As we have already discussed in connection with Figs. 3 and 4 above, the strength of the peak at 1.12 a.u. in  $J_{\text{mag}}(p)$  is related to the extent to which magnetic electrons on B-sites develop phase coherence via the admixture parameter  $f$  on NN Fe B-sites. It may then be argued that the quantity  $A$  defined via the integral of Eq. 4 is a measure of the area under the peak in  $J_{\text{mag}}(p)$ , and thus of the number of magnetic electrons participating in this coherence process [34].

Fig. 5 shows that the value of  $A$  increases systematically in going from the 10K to the 300K dataset. Interestingly, this behavior of  $A$  correlates with that of the admixture parameter  $f$  discussed above in connection with Figs. 3 and 4 in that, like  $A$ , the parameter  $f$  also increases with temperature. In other words, the Verwey

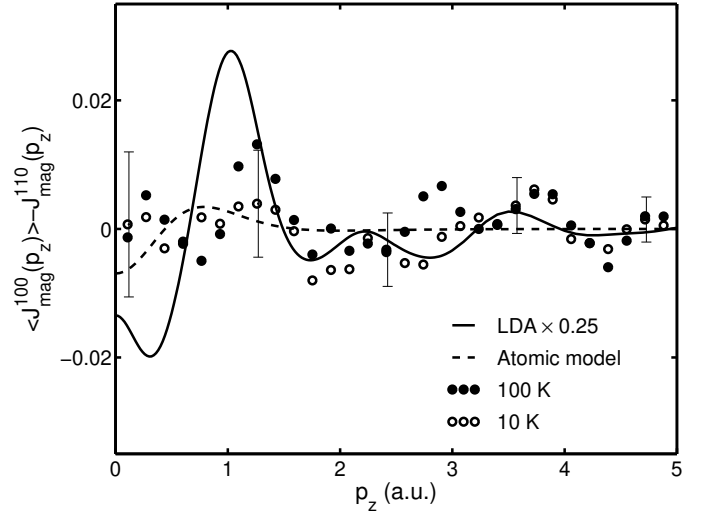


FIG. 4: Anisotropy of the MCP defined as  $J_{\text{mag}} = \frac{J_{\text{mag}}^{[100]} - J_{\text{mag}}^{[110]}}{J_{\text{mag}}^{[100]} + J_{\text{mag}}^{[110]}}$ , where the areas under all profiles are normalized to one. Experimental results for the 10K and 100K datasets are compared with the simple atomic analysis of Ref. [17]. The LDA curve is reproduced from Fig. 3 for reference.

transition is accompanied by a change in the character of the ground state wavefunction such that the wavefunction becomes significantly more delocalized on Fe B-sites above  $T_V$ . Notably, the present analysis suggests that the B-site is involved in the change in valence across the Verwey transition as in Ref. [35], and not the A-site as argued in Ref. [36] recently. Positron annihilation experiments [37, 38], which also give information on spin-resolved momentum density, have revealed covalency effects between Fe and O atoms but have failed to detect significant changes at  $T_V$ . This result however may reflect the tendency of the positron to sample mostly O-ions and interstitial spaces rather than the Fe-ions.

In conclusion, we have presented magnetic Compton scattering measurements on a magnetite single crystal, together with corresponding predictions of the MCP within the conventional band picture. An accurate value of the unpaired spin moment  $S$  is thus obtained directly over a wide temperature range. For example, at 10 K  $S$  has clearly a non integer value of  $3.54 \pm 0.05 \mu_B$ /formula unit for the magnetic field along [100] demonstrating a non vanishing spin-orbit coupling. The ground state of magnetite is shown to be remarkably sensitive to the direction of the external magnetic field around the Verwey transition and to display an anomalous magnetic moment, which may be a manifestation of a large degeneracy and associated geometrical frustration in the spinel lattice. The amplitude of the anisotropy of the MCP is shown to increase with temperature. We argue on this basis that the ground state wavefunction in the system

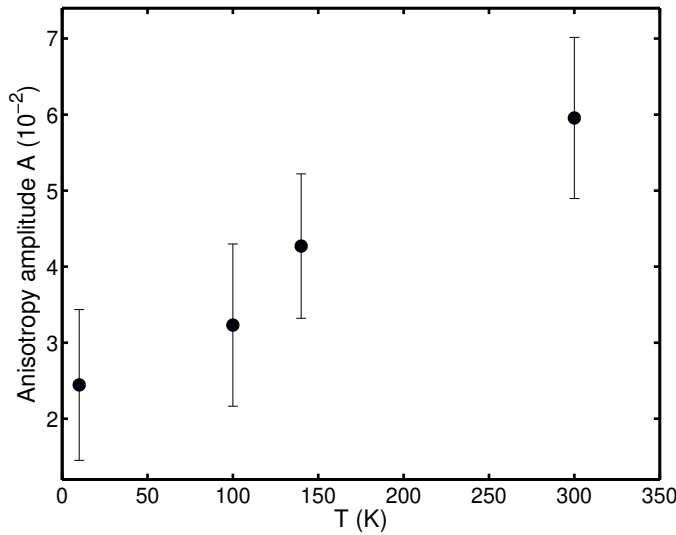


FIG. 5: Amplitude  $A$  of the MCP anisotropy obtained from Eqs. 3 and 4 as a function of temperature.

becomes delocalized on Fe B-sites above  $T_v$ .

We acknowledge discussions with R.S. Markiewicz, Hsin Lin and E. Tosatti, the support of the U.S.D.O.E. contracts DE-AC 03-76SF 00098, DE-FG 02-07ER 46352 and the U.S. DOE support of the Advanced Photon Source at Argonne National Laboratory. We benefited from the allocation of supercomputer time at NERSC, Northeastern University's Advanced Scientific Computation Center (ASCC) and the Stichting NCF (Foundation National Computer Facilities).

[1] E.J.W. Verwey, *Nature* 144, 327 (1939).  
 [2] E.J.W. Verwey and P.W. Haayman, *Physica* 8, 979 (1941).  
 [3] P. Novak, H. Stepankova, J. Englich, J. Kohout and V. A.M. Brabers, *Phys. Rev. B* 61, 1256 (2000).  
 [4] F. Waltz, *J. Phys.: Condens. Matter* 14 R285 (2002).  
 [5] J. Garcia and G. Subias, *J. Phys.: Condens. Matter* 16 R145 (2004).  
 [6] M. Coey, *Nature* 430, 327 (2004).  
 [7] P.G. Radaelli, *New J. Phys.* 7, 53 (2005).  
 [8] Yanase and K. Siratori, *J. Phys. Soc. Japan* 53, 312 (1984).  
 [9] Z. Zhang and S. Satpathy, *Phys. Rev. B* 44, 13319 (1991).  
 [10] A. Yanase and N. Hamada, *J. Phys. Soc. Japan* 68, 1607 (1999).  
 [11] M. J. Cooper, P.E. Mijarends, N. Shiotani, N. Sakai and A. Bansil, in *X-Ray Compton Scattering*, Oxford University Press (2004) and references therein.  
 [12] D.J. Huang, C.F. Chang, H.-T. Jeng, G.Y. Guo, H.-J. Lin, W.B. Wu, H.C. Ku, A. Fujimori, Y. Takahashi, and C.T. Chen, *Phys. Rev. Lett.* 93, 077204 (2004).  
 [13] E. Goering, S. Gold, M. Lafkioti and G. Schutz, *Europhys. Lett.* 73, 97 (2006).

[14] E. Goering, M. Lafkioti, and S. Gold, *Phys. Rev. Lett.* 96, 039701 (2006).  
 [15] D.J. Huang, H.-J. Lin, and C.T. Chen, *Phys. Rev. Lett.* 96, 039702 (2006).  
 [16] Yinwan Li, P.A. Montano, J.F. Mitchell, B. Barbiellini, P.E. Mijarends, S. Kaprzyk, and A. Bansil, *Phys. Rev. Lett.* 93, 207206 (2004).  
 [17] P.A. Montano, Yinwan Li, J.F. Mitchell, B. Barbiellini, P.E. Mijarends, S. Kaprzyk, and A. Bansil, *J. Phys. Chem. Solids* 65, 1999 (2004).  
 [18] P.A. Montano, Yinwan Li, U. Ruett, M.A. Beno, G. Jennings and C.W. Kimball, *Proc. SPIE* 3773, 262 (1999).  
 [19] A. Bansil, S. Kaprzyk, P.E. Mijarends and J. Tobola, *Phys. Rev. B* 60, 13396 (1999).  
 [20] P.E. Mijarends and A. Bansil, in *Positron Spectroscopy of Solids*, eds. A. Dupasquier and A.P. Mills (IOS Press, Amsterdam, 1995), p. 25, and references therein.  
 [21] R. A. Ragon, *Phys. Rev. B* 46, 5328 (1992).  
 [22] R. J. M. Queeney, M. Yethiraj, W. Montfrooij, J. S. Gardner, P. Metcalfe, and J. M. Honig, *Phys. Rev. B* 73, 174409 (2006).  
 [23] K. Abe, Y. Miyamoto and S. Chikazumi, *J. Phys. Soc. Japan* 41, 1894 (1976).  
 [24] M. Matsui, S. Todo and S. Chikazumi, *J. Phys. Soc. Japan* 43, 47 (1977).  
 [25] H. Uzu and A. Tanaka, *J. Phys. Soc. Japan* 75, 043704 (2006).  
 [26] H. Uzu, private communication.  
 [27] L. Neel, *Ann. Phys. (Paris)* 3, 137 (1948).  
 [28] The Compton profile anisotropy is often invoked to highlight relatively small oscillating terms reflecting coherence properties of the ground state wavefunction. See e.g. E.D. Isaacs, A. Shukla, P.M. Platzman, D.R. Hamann, B. Barbiellini, and C.A. Tulk, *Phys. Rev. Lett.* 82, 600 (1999). In magnetite, the [100] profile is dominated by atomic d-like behavior and it does not contain a significant interference term from the nearest neighbor Fe-Fe overlap. Therefore, in the [100]-[110] difference profile, the [100] profile essentially allows us to subtract an underlying atomic contribution to the [110] profile and to thus highlight interference effects in the [110] profile. E  
 [29] We have also obtained  $J_{mag}$  where the average  $J_{mag}^{[100]}$  was taken over just the two high (140K and 300K) or the two low (10K and 100K) temperature datasets. The resulting anisotropy is quite similar to that shown in Figs. 3 and 4 where all four datasets are employed in the averaging process, indicating that our use of  $J_{mag}^{[100]}$  as background does not introduce any spurious features in the anisotropy defined by Eq. 3.  
 [30] T. Chiba, *J. Chem. Phys.* 64, 1182 (1975).  
 [31] The other Fe-Fe distances  $d_{BA} = 6.58$  a.u. and  $d_{AA} = 6.88$  a.u. do not yield the main peak at 1.12 a.u. Only the distance  $d_{BB} = 5.61$  a.u. yields the good fit shown in Fig. 3.  
 [32] The error in our values of  $f$  is estimated to be 0.02.  
 [33] The temperature dependence of  $A$  shown in Fig. 5 is not sensitive to the value of the cut-off momentum  $p_{max}$ .  
 [34] The factor of  $l=2$  in Eq. 4 accounts for the presence of positive excursions in  $J_{mag}(p)$  (in particular the peak at 1.12 a.u.) which involve the same area as the negative contributions.  
 [35] E. Nazarenko, J. E. Lorenzo, Y. Joly, J. L. Hodeau,

- D. M. Annix and C. M. Arin, Phys. Rev. Lett. 97, 056403 (2006).
- [36] G. K. H. Rozenberg, M. P. Pasternak, W. M. Xu, Y. Amiel, M. Han and, M. Ambroage, R. D. Taylor, and R. Jeanloz, Phys. Rev. Lett. 96, 045705 (2006).
- [37] P. E. M. J. Harelds and R. M. Singru, Appl. Phys. 4, 303 (1974).
- [38] M. Biasini, T. Chiba, A. A. Manuel, T. Akahane and A. Yanase, Materials Science Forum 255-257, 515 (1997).